Stacking-velocity tomography with borehole constraints for tilted TI media

Xiaoxiang Wang & Ilya Tsvankin
Center for Wave Phenomena, Geophysics Department, Colorado School of Mines, Golden, Colorado 80401

ABSTRACT
Transversely isotropic models with a tilted symmetry axis (TTI) play an increasingly important role in seismic imaging, especially near salt bodies and in active tectonic areas. Here, we present a 2D parameter-estimation methodology for TTI media based on combining P-wave normal-moveout (NMO) velocities, zero-offset traveltimes, and reflection time slopes with borehole data that include the vertical group velocities as well as the reflector depths and dips.
For a dipping TTI layer with the symmetry axis confined to the dip plane of the reflector, estimation of the symmetry-direction velocity V_{P0}, the anisotropy parameters ϵ and δ, and the tilt ν of the symmetry axis proves to be ambiguous despite the borehole constraints. If the symmetry axis is orthogonal to the reflector (a model typical for dipping shale layers), V_{P0} and δ can be recovered with high accuracy, even when the symmetry axis deviates by $\pm 5^\circ$ from the reflector normal. The parameter ϵ, however, cannot be constrained for dips smaller than 60° without using nonhyperbolic moveout.
To invert for the interval parameters of layered TTI media, we apply 2D stacking-velocity tomography supplemented with the same borehole constraints. The dip planes in all layers are assumed to be aligned; also, the symmetry axis is set orthogonal to the reflector in each layer, which helps to avoid ambiguity caused by an unknown tilt ν. Synthetic tests confirm that estimation of the interval parameters V_{P0} and δ remains stable in the presence of Gaussian noise in the input data. Our algorithm can be used to build an accurate initial TTI model for post-migration reflection tomography and other techniques that employ migration velocity analysis.

Key words: transverse isotropy, tilted axis, TTI, moveout inversion, interval parameters, stacking velocity, dipping reflectors, tomography, borehole data

1 INTRODUCTION

Ignoring anisotropy in P-wave processing causes imaging and interpretation errors, such as mispositioning of horizontal and dipping reflectors (e.g., Alkhalifah & Larner, 1994; Alkhalifah *et al.*, 1996; Vestrum *et al.*, 1999). While many widely used migration algorithms have been extended to transversely isotropic (TI) media, constructing an accurate anisotropic velocity model remains a challenging problem. For TI models with a vertical symmetry axis (VTI), the depth-domain P-wave velocity field is controlled by the vertical velocity V_{P0} and the Thomsen (1986) parameters ϵ and δ. To resolve all three parameters individually, P-wave moveout typically has to be combined with shear modes (SS- or PS-waves) or borehole data (Tsvankin & Grechka, 2000; Sexton & Williamson, 1998).

Vertical transverse isotropy has proved to be adequate for most horizontally stratified, unfractured sediments. However, in progradational clastic or carbonate sequences, as well as in the presence of obliquely dipping fractures, the symmetry axis is tilted (Figure 1). Also, TI with a tilted symmetry axis (TTI) is an appropriate model for dipping shale layers near salt domes and in fold-and-thrust belts such as the Canadian Foothills (Isaac & Lawton, 1999; Vestrum *et al.*, 1999; Charles

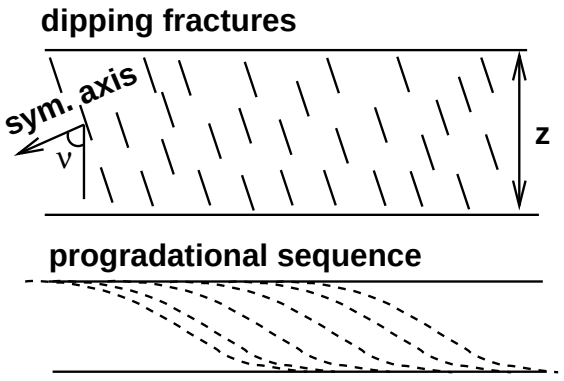

Figure 1. TI layer with a tilted symmetry axis describes progradational sequences and a system of obliquely dipping, penny-shaped fractures embedded in isotropic host rock (after Dewangan & Tsvankin, 2006a).

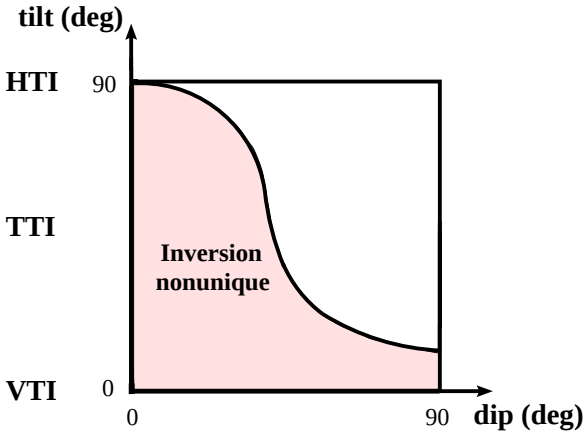

Figure 2. Illustration of the uniqueness of depth-domain parameter estimation for TI media using multicomponent data (after Grechka *et al.*, 2002a). The tilt and azimuth of the symmetry axis are assumed to be unknown, even for VTI and HTI models.

et al., 2008; Huang *et al.*, 2008; Behera & Tsvankin, 2009). The parameters V_{P0}, ϵ, and δ for TTI media are defined in the rotated coordinate system with respect to the symmetry axis, whose orientation is described by the tilt angle ν with the vertical and the azimuth β.

In principle, the symmetry-axis orientation and the interval parameters V_{P0}, ϵ, and δ of a TTI layer can be estimated from wide-azimuth P-wave data (Grechka & Tsvankin, 2000), if the medium is not close to elliptical (i.e., $\epsilon \neq \delta$). Stable inversion, however, requires at least two NMO ellipses from interfaces with different orientations (e.g., a horizontal and a dipping reflector). Also the tilt ν of the symmetry axis has to exceed 30° and the reflector dip ϕ should be between 30° and 80° (Grechka & Tsvankin, 2000). If shear data are available, the addition of the SV-wave NMO ellipse from a horizontal reflector helps to increase the inversion accuracy and makes parameter estimation possible for elliptically anisotropic media. Still, combining horizontal SV-wave events with P-wave data does not remove the above constraints on ν and ϕ (Grechka & Tsvankin, 2000).

Grechka *et al.* (2002a) developed a multicomponent tomographic algorithm for interval parameter estimation in layered TI media using wide-azimuth PP and PSV (or SVSV) reflection data. For relatively large tilt angles ν and reflector dips, multicomponent, multiazimuth reflection data can be used to build anisotropic models for depth processing. However, parameter estimation is still ambiguous for a wide range of small and moderate angles ν and ϕ (Figure 2).

To carry out parameter estimation for a horizontal TTI layer, Dewangan & Tsvankin (2006a) applied the PP+PS=SS method (Grechka & Tsvankin, 2002; Grechka & Dewangan, 2003) to reflection traveltimes of PP- and PS-waves. They implemented nonlinear inversion of the NMO velocities and zero-offset traveltimes of the recorded PP-waves and computed SS-waves combined with the moveout-asymmetry attributes of the PS(PSV)-wave. ⋆ The method of Dewangan & Tsvankin (2006a) remains accurate for a wide range of tilts, except for "quasi-VTI" models with $\nu < 10°$.

Dewangan & Tsvankin (2006b) extended this algorithm to a dipping TTI layer with the symmetry axis orthogonal to the layer's bottom. In that model, the moveout asymmetry of PSV-waves is caused not just by the tilted symmetry axis, but also by the reflector dip. Despite the constraint on the symmetry axis, the parameter estimation is stable only for large tilts ($\nu > 40°$), with the anisotropy parameter δ constrained more tightly than ϵ. If high-quality PS data are available, the inversion becomes feasible for moderate tilts ($25° < \nu < 40°$).

Although PS-waves provide valuable information for velocity model building in the depth domain, they are seldom acquired in exploration. Also, processing of mode-converted data is much more difficult than that of pure PP reflections, and it is difficult to identify the pure and converted events from the same interface. Moreover, implementation of the multicomponent inversion algorithms is hindered by the strong spatial amplitude variations and phase reversals of converted waves.

Here, we present a 2D inversion methodology for TTI media based on combining conventional-spread P-wave moveout with borehole information. P-wave NMO velocities and zero-offset traveltimes are supplemented not just with the velocity along the borehole and re-

⋆The moveout of PS-waves is asymmetric if the traveltime does not stay the same when the source and receiver are interchanged. In a horizontal TTI layer, this asymmetry is caused by the tilt of the symmetry axis.

flector depths, but also with the dips of all interfaces. First, we introduce a semi-analytic inversion procedure for a single TTI layer above a dipping interface and show that the medium parameters cannot be resolved without constraining the tilt of the symmetry axis. Then we develop joint tomographic inversion of moveout and borehole data for a stack of TTI layers with the symmetry axis orthogonal to the layer boundaries. Synthetic tests with a realistic level of Gaussian noise illustrate the stability of estimating the interval parameters V_{P0}, ϵ, and δ.

2 INVERSION FOR A SINGLE TTI LAYER

We start by considering the simple model of a homogeneous TTI layer above a planar dipping reflector. To make the problem 2D, the symmetry axis is assumed to be confined to the dip plane. The tilt angle ν is taken positive, if the symmetry axis is rotated counter-clockwise from the vertical. P-wave surface data provide the zero-offset reflection time t_0, the reflection slope (horizontal slowness) p on the zero-offset time section, and the NMO velocity $V_{\rm nmo}$. Because the layer is homogeneous, it is sufficient to have the estimates of t_0, p, and $V_{\rm nmo}$ for a single common midpoint (CMP). At a location where a vertical well is available, we can measure the P-wave vertical group velocity along with the depth and dip of the reflector.

2.1 Arbitrary axis orientation

2.1.1 Inversion methodology

The exact P-wave phase-velocity function in TI media expressed through the Thomsen parameters is given by (Tsvankin, 1996, 2005)

$$\frac{V^2}{V_{P0}^2} = 1 + \epsilon \sin^2\theta - \frac{f}{2} + \frac{f}{2}\sqrt{1 + \frac{4\sin^2\theta}{f}(2\delta\cos^2\theta - \epsilon\cos 2\theta) + \frac{4\epsilon^2\sin^4\theta}{f^2}}\,, \tag{1}$$

where θ is the phase angle with the symmetry axis (assumed to be positive for counter-clockwise rotation), V_{P0} is the symmetry-direction velocity, and

$$f \equiv 1 - \frac{V_{S0}^2}{V_{P0}^2}\,; \tag{2}$$

V_{S0} is the symmetry-direction velocity of S-waves. Because the influence of V_{S0} on P-wave kinematics is negligible, the value of f can be set to a constant using a typical V_{P0}/V_{S0} ratio (e.g., $V_{P0}/V_{S0} = 2$). Therefore, the phase velocity V represents a function of the four medium parameters (V_{P0}, ϵ, δ, and ν) and the phase angle $\tilde\theta$ with the vertical:

$$V = f_1(V_{P0}, \epsilon, \delta, \tilde\theta, \nu)\,; \tag{3}$$

the phase angle with the symmetry axis in equation 1 is $\theta = \tilde\theta - \nu$.

For the zero-offset reflection, the phase-velocity (slowness) vector is perpendicular to the reflector, and the phase angle with the vertical $\tilde\theta$ is equal to the dip ϕ_w (Figure 3a; the subscript "w" denotes well data). The phase velocity for the zero-offset reflection can be computed through the known values of ϕ_w and p as

$$V_{\phi_w} = \frac{\sin\phi_w}{p}\,. \tag{4}$$

Substituting equation 4 into equation 3 yields

$$f_1(V_{P0}, \epsilon, \delta, \phi_w, \nu) = \frac{\sin\phi_w}{p}\,. \tag{5}$$

The P-wave group velocity V_G in TI media can be found as a function of the phase velocity V and its derivative with respect to θ (e.g., Tsvankin, 2005):

$$V_G = V\sqrt{1 + \left(\frac{1}{V}\frac{dV}{d\theta}\right)^2}\,. \tag{6}$$

Therefore, V_G represents a function (different from f_1) of the parameters V_{P0}, ϵ, δ, $\tilde\theta$, and ν:

$$V_G = f_2(V_{P0}, \epsilon, \delta, \tilde\theta, \nu)\,. \tag{7}$$

The P-wave group angle ψ with the symmetry axis is also controlled by the angle-dependent phase velocity (e.g., Tsvankin, 2005):

$$\tan\psi = \frac{\tan\theta + \frac{1}{V}\frac{dV}{d\theta}}{1 - \frac{\tan\theta}{V}\frac{dV}{d\theta}}\,. \tag{8}$$

Therefore, the angle $\tilde\psi$ with the vertical in a TTI layer can be rewritten as

$$\tilde\psi = f_3(V_{P0}, \epsilon, \delta, \tilde\theta, \nu)\,. \tag{9}$$

For the zero-offset reflection, the phase angle $\tilde\theta = \phi_w$ (Figure 3a), so

$$V_{G0} = f_2(V_{P0}, \epsilon, \delta, \phi_w, \nu)\,, \tag{10}$$

and the group angle with the vertical is

$$\tilde\psi_0 = f_3(V_{P0}, \epsilon, \delta, \phi_w, \nu)\,. \tag{11}$$

The length of the zero-offset raypath (AB in Figure 3a) can be calculated from the vertical thickness z_w of the layer and the angles ϕ_w and $\tilde\psi_0$ (Figure 3a). AB can also be expressed through the two-way zero-offset reflection time t_0 and the group velocity given by equation 10:

$$\frac{z_w\cos\phi_w}{\cos(\tilde\psi_0 - \phi_w)} = \frac{V_{G0}\,t_0}{2}\,; \tag{12}$$

$\tilde\psi_0$ is found from equation 11. Note that if the CMP is displaced from the well by a known distance, equation 12 can be modified accordingly. Hence, we have constructed two equations (5 and 12) for the four unknown parameters.

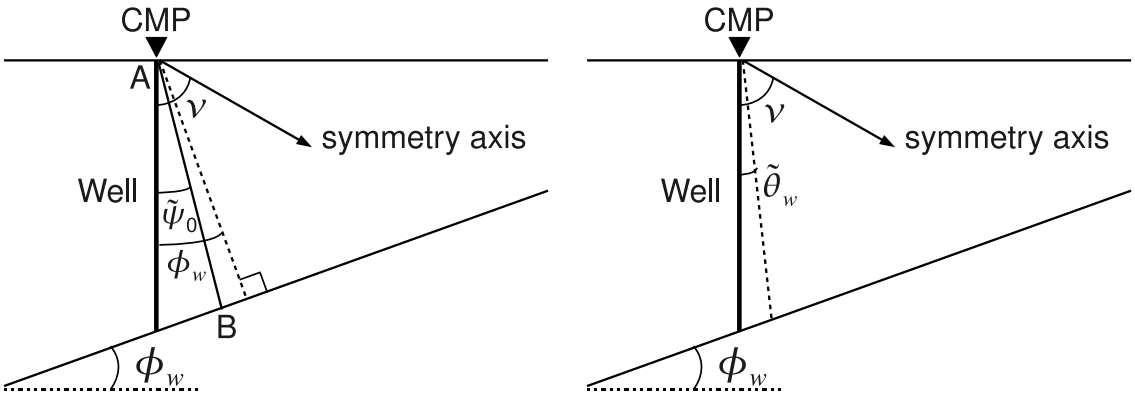

Figure 3. Dipping TTI layer with the CMP at the head of a vertical well. The arrow marks the symmetry axis; the reflector dip is ϕ_w. a) AB is the zero-offset raypath; the group and phase angles of the zero-offset ray with the vertical are $\tilde{\psi}_0$ and ϕ_w, respectively. b) The phase-velocity vector of the vertical ray makes the angle $\tilde{\theta}_w$ with the vertical.

For the P-wave propagating along the well, the group angle with the vertical is zero, but the corresponding phase angle $\tilde{\theta}_w$ is unknown (Figure 3b). Applying equations 7 and 9 to the vertical ray gives

$$f_2(V_{P0}, \epsilon, \delta, \tilde{\theta}_w, \nu) = V_{Gw}\,, \tag{13}$$

$$f_3(V_{P0}, \epsilon, \delta, \tilde{\theta}_w, \nu) = 0\,. \tag{14}$$

The pure-mode NMO velocity for 2D wave propagation in a symmetry plane can be expressed as a function of the phase velocity $V(\theta)$ and reflector dip ϕ (Tsvankin, 2005):

$$V_{\rm nmo}(\phi) = \frac{V(\phi)}{\cos\phi}\frac{\sqrt{1+\frac{1}{V(\phi)}\frac{d^2V}{d\theta^2}\Big|_{\theta=\phi}}}{1-\frac{\tan\phi}{V(\phi)}\frac{dV}{d\theta}\Big|_{\theta=\phi}}\,. \tag{15}$$

In a dipping TTI layer (Figure 3), the phase velocity and its derivatives in equation 15 should be computed at the phase angle $\theta_0 = \phi_w - \nu$ with the symmetry axis. Alternatively, it is possible to obtain $V_{\rm nmo}$ as a function of the known reflection slope p. Therefore, equation 15 provides another constraint on the medium parameters:

$$V_{\rm nmo} = f_4(V_{P0}, \epsilon, \delta, \phi_w, \nu)\,. \tag{16}$$

Therefore, we derived five equations (5, 12, 13, 14, and 16) to be inverted for the four TTI parameters $(V_{P0}, \epsilon, \delta, \nu)$ and the phase angle $\tilde{\theta}_w$ corresponding to the vertical ray:

$$f_1(V_{P0}, \epsilon, \delta, \phi_w, \nu) = \frac{\sin\phi_w}{p}\,; \tag{17}$$

$$\frac{z_w\cos\phi_w}{\cos\left[f_3(V_{P0}, \epsilon, \delta, \phi_w, \nu) - \phi_w\right]} = \frac{t_0\, f_2(V_{P0}, \epsilon, \delta, \phi_w, \nu)}{2}\,; \tag{18}$$

$$f_2(V_{P0}, \epsilon, \delta, \tilde{\theta}_w, \nu) = V_{Gw}\,; \tag{19}$$

$$f_3(V_{P0}, \epsilon, \delta, \tilde{\theta}_w, \nu) = 0\,; \tag{20}$$

$$f_4(V_{P0}, \epsilon, \delta, \phi_w, \nu) = V_{\rm nmo}\,. \tag{21}$$

For VTI media (i.e., $\nu = 0°$), V_{P0} is obtained directly from the well measurement ($\tilde{\theta}_w = 0°$, $V_{P0} = V_{Gw}$); then ϵ and δ are found from equations 17 and 21. If the dip is unknown, the parameters ϵ, δ, and ϕ_w can be estimated from equations 17, 18, and 21. Here, however, we concentrate on the inversion for nonzero tilt.

2.1.2 Synthetic example

Although the number of equations is equal to the number of unknowns, equations 17–21 form a nonlinear system, which is not guaranteed to have a unique solution. To evaluate the feasibility of the inversion, we computed the input data (p, t_0, $V_{\rm nmo}$, and V_{Gw}) from the exact equations and contaminated them by Gaussian noise with the standard deviations equal to 1% for p and t_0, and 2% for $V_{\rm nmo}$ and V_{Gw}. The reflector dip ϕ_w and depth z_w were assumed to be known exactly, and the starting model was isotropic (i.e., $\epsilon = \delta = 0$). Table 1 shows the inversion results for typical TTI parameters using 100 realizations of the input data. Despite the constraints provided by borehole data, the inversion proves

	Actual	Estimated	
		mean	sd
V_{P0} (km/s)	2.50	2.92	0.25
ϵ	0.25	0.15	0.77
δ	0.10	-0.14	0.14
ν (°)	50	-20	33
Dip (°)	30	–	–
Depth (km)	1	–	–

Table 1. Actual and estimated parameters of a TTI layer. The dip and depth are measured at the well location. The input data were contaminated by Gaussian noise with the standard deviations equal to 1% for p and t_0, and 2% for $V_{\rm nmo}$ and V_{Gw}. The standard deviations and mean values of the inverted parameters are denoted by "sd" and "mean," respectively.

to be highly unstable, with small errors in the data producing large distortions in the estimated parameters. This instability is partially caused by the nonlinear dependence of the phase velocity V on the tilt ν (Grechka *et al.*, 2002a). Similar results were obtained for a wide range of model parameters.

2.2 Symmetry axis orthogonal to the reflector

If TTI symmetry is associated with dipping shale layers, the symmetry axis is typically orthogonal to the layer boundaries (Isaac & Lawton, 1999; Vestrum *et al.*, 1999; Charles *et al.*, 2008). Fixing the orientation of the symmetry axis helps to overcome the nonuniqueness of the inversion procedure (Grechka *et al.*, 2002a; Zhou *et al.*, 2008; Behera & Tsvankin, 2009).

2.2.1 Inversion methodology

If the symmetry axis is orthogonal to the reflector, the tilt ν is equal to the reflector dip ϕ_w measured in the well. Also, the phase-velocity vector of the zero-offset reflection is parallel to the symmetry axis, and the velocity V_{P0} can be obtained directly from surface data and the dip ϕ_w:

$$V_{P0} = \frac{\sin\phi_w}{p}\,. \tag{22}$$

The NMO velocity for $\nu = \phi_w$ is given by the isotropic cosine-of-dip relationship (Tsvankin, 2005):

$$V_{\rm nmo} = \frac{V_{\rm nmo}(0)}{\cos\phi_w}\,, \tag{23}$$

where $V_{\rm nmo}(0) = V_{P0}\sqrt{1+2\delta}$. Since V_{P0} is already known, equation 23 constrains the parameter δ.

Because the group and phase velocities in the symmetry direction coincide, equation 18 contains only known quantities and can be used to check the validity of the model. Therefore, the inverse problem reduces to estimating the parameters ϵ and $\tilde{\theta}_w$ from the vertical group velocity (i.e., from equations 19 and 20):

$$f_2(V_{P0},\epsilon,\delta,\tilde{\theta}_w,\phi_w) = V_{Gw}\,; \tag{24}$$

$$f_3(V_{P0},\epsilon,\delta,\tilde{\theta}_w,\phi_w) = 0\,. \tag{25}$$

Evidently, when $\nu = \phi_w$, the inversion equations do not include z_w and are independent of the CMP location. Moreover, if the well is not vertical but its inclination is known, equations 24 and 25 retain the same form with a nonzero group angle on the right-hand side of equation 25.

2.2.2 Synthetic examples

First, we perform a test on noise-contaminated data for a model with $\nu = \phi_w = 30^\circ$ and typical values of the Thomsen parameters (Figure 4a). The parameters V_{P0} and δ can be estimated with high accuracy; the mean value of V_{P0} is 2.50 km/s with the standard deviation 1%; the mean value of δ is 0.10 with the standard deviation 0.03. However, the parameter ϵ is practically unconstrained (the standard deviation is 1.37). The instability in estimating ϵ can be explained using the linearized weak-anisotropy approximation. For weak anisotropy, the phase and group velocities coincide (Thomsen, 1986), and for the vertical ray

$$V_{Gw} = V_{P0}(1+\delta\sin^2\phi_w\cos^2\phi_w + \epsilon\sin^4\phi_w)\,. \tag{26}$$

For moderate dips, such as $\phi_w = 30^\circ$ used in the test, the contribution of ϵ is much smaller than that of δ because ϵ is multiplied with $\sin^4\phi_w$.

We repeated the test for a range of dips with the results listed in Table 2. The estimates of V_{P0} and δ are sufficiently accurate, with small (and practically constant) standard deviations for all dips. The errors in the parameter ϵ, however, are much larger; to resolve ϵ from the vertical group velocity, the dip (and tilt) should reach at least 60°. Our algorithm operates with NMO velocity, which controls reflection moveout for offset-to-depth ratios limited by unity. If long-spread P-wave data (with the offset-to-depth ratio reaching two) are available, it is possible to estimate ϵ from nonhyperbolic moveout (Behera & Tsvankin, 2009).

If the symmetry axis is not orthogonal to the reflector, the algorithm based on setting $\nu = \phi_w$ produces errors in the inverted parameters. However, for typical moderate magnitudes of ϵ and δ ($|\epsilon| \le 0.5$; $|\delta| \le 0.3$), the errors in V_{P0} and δ remain small, if the symmetry axis deviates from the reflector normal by less than 5° and the dip ranges from 5° to 50° (Table 3). For example, we computed the input data with the actual tilt $\nu = 15^\circ$ and dip $\phi_w = 20^\circ$, then obtained the parameters $V_{P0} = 2.5\,$km/s and $\delta = 0.11$ under the as-

Dip (°)	V_{P0}		δ		ϵ	
	sd (%)	mean (km/s)	sd	mean	sd	mean
5	1	2.50	0.03	0.10	1724	251
10	1	2.50	0.03	0.10	854	282
20	1	2.50	0.03	0.10	48	14.6
30	1	2.50	0.03	0.10	1.37	0.64
40	1	2.50	0.03	0.10	0.29	0.31
50	1	2.50	0.03	0.10	0.13	0.27
60	1	2.50	0.03	0.10	0.07	0.26
70	1	2.50	0.03	0.10	0.05	0.25

Table 2. Inversion results for a single TTI layer with the symmetry axis perpendicular to its bottom. The medium parameters are $V_{P0} = 2.5$ km/s, $\delta = 0.10$, and $\epsilon = 0.25$. The data were contaminated by Gaussian noise with the standard deviations equal to 1% for p, and 2% for $V_{\rm nmo}$ and V_{Gw}.

Dip (°)	ν (°)	V_{P0}		δ	
		sd (%)	mean (km/s)	sd	mean
5	0	1	2.51	0.03	0.11
5	10	1	2.51	0.03	0.10
20	15	1	2.50	0.03	0.11
20	25	1	2.50	0.03	0.10
40	35	1	2.50	0.03	0.12
40	45	1	2.50	0.03	0.09
60	55	1	2.50	0.03	0.15
60	65	1	2.50	0.03	0.07

Table 3. Inversion results for a TTI layer with the symmetry axis deviating from the reflector normal by ±5°. The parameters V_{P0} and δ are obtained under the assumption that the symmetry axis is orthogonal to the reflector. The input data were contaminated by Gaussian noise with the standard deviations equal to 1% for p, and 2% for $V_{\rm nmo}$ and V_{Gw}.

sumption that $\nu = \phi_w = 20°$. The inversion results become more distorted for strong anisotropy because the value of $\sin\phi_w/p$ differs more significantly from the actual symmetry-direction velocity V_{P0}.

3 TOMOGRAPHIC INVERSION FOR LAYERED TTI MEDIA

In the previous section we demonstrated the feasibility of inverting P-wave moveout and borehole measurements for the parameters of a single TTI layer with the symmetry axis orthogonal to its bottom. Here, we present a tomographic algorithm for interval parameter estimation in layered TTI media using reflection and borehole data.

The model is composed of homogeneous TTI layers separated by planar dipping boundaries with the same azimuth of the dip plane. The symmetry axis in each layer is perpendicular to its bottom, which makes wave propagation two-dimensional. Then the model vector for an N-layered medium can be written as

$$\widetilde{m} = \{V_{P0}^{(n)}, \epsilon^{(n)}, \delta^{(n)}, \nu^{(n)}\}\,, \quad (n = 1, 2, \ldots, N)\,. \qquad (27)$$

The data vector takes the form

$$\widetilde{d} = \{t_0(n), p(n), V_{\rm nmo}(n), z_w^{(n)}, \phi_w^{(n)}, V_{Gw}^{(n)}\}\,,$$
$$(n = 1, 2, \ldots, N)\,, \qquad (28)$$

where $t_0(n)$, $p(n)$, and $V_{\rm nmo}(n)$ are the effective values for the n-th reflector measured from reflection data, $z_w^{(n)}$ and $\phi_w^{(n)}$ are the depth and dip of the n-th reflector, respectively, at the well location, and $V_{Gw}^{(n)}$ is the interval vertical group velocity in the n-th layer.

3.1 Inversion methodology

The algorithm generalizes the inversion scheme for a single TTI layer discussed above, and represents a modification of stacking-velocity tomography introduced for VTI media by Grechka *et al.* (2002b). Since the tilt $\nu^{(n)}$ of the symmetry axis in each layer is equal to the dip $\phi_w^{(n)}$, there is a total of $3N$ unknown parameters $\{V_{P0}^{(n)}$, $\epsilon^{(n)}$, $\delta^{(n)}\}$ for the N-layered TTI medium. The model geometry can be fully reconstructed from the known depths and dips of the interfaces.

For a given set of the trial interval parameters $\widetilde{m}$ (equation 27), we compute the NMO velocities $V_{\rm nmo,calc}(n)$ using the Dix-type averaging procedure based on tracing the zero-offset ray (Grechka *et al.*, 2002b). The interval vertical group velocities $V_{Gw}^{(n)}$ are

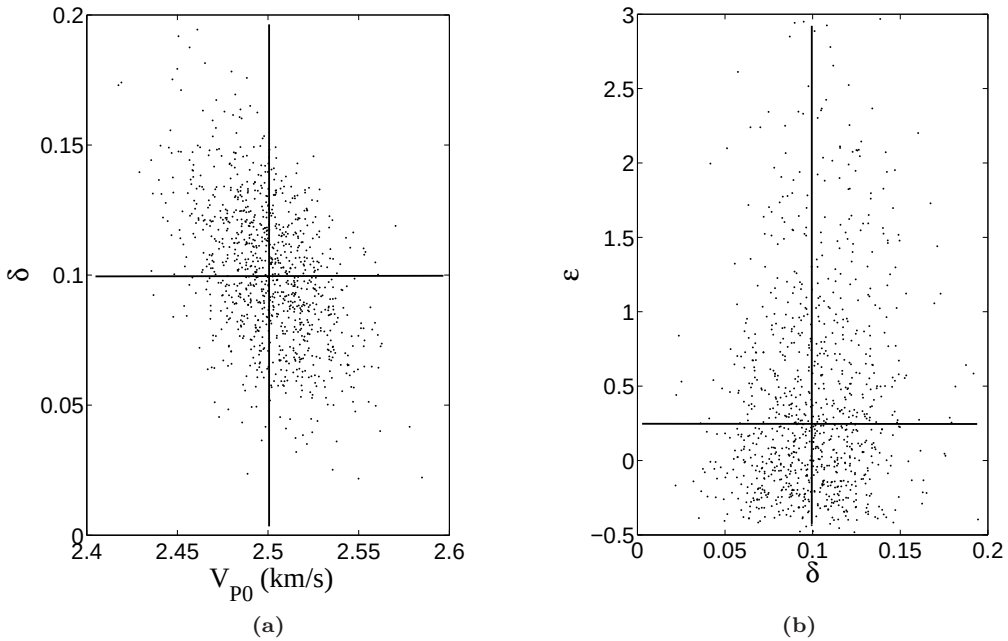

Figure 4. Inversion results (dots) for a TTI layer with the symmetry axis orthogonal to its bottom. The inversion was carried out for 1000 realizations of input data contaminated by Gaussian noise with the standard deviations equal to 1% for the reflection slope p and 2% for $V_{\rm nmo}$ and V_{Gw}. Due to the large standard deviation (1.37) of ϵ, the ϵ-axis on plot (b) is clipped. The actual parameter values are marked by the crosses. The starting model was isotropic.

also obtained by ray tracing in the trial model. Fitting the interval velocity $V_{Gw}^{(n)}$ is equivalent to solving equations 24 and 25 for a single layer because the phase angle $\tilde{\theta}_w$ for the vertical ray is obtained from the trial medium parameters.

Reflection slopes in layered media cannot yield the interval symmetry-direction velocities directly (as in equation 22). Instead, we use the slopes $p(n)$ and zero-offset traveltimes $t_0(n)$ (equation 28) to construct the one-way zero-offset rays for the trial TTI parameters and compute the "trial" reflector depths in the well. For the first layer, the vertical slowness of the zero-offset ray and the slowness vector as a whole can be computed from the trial parameters $\widetilde{m}_1$ and the horizontal slowness $p(1)$ using the Christoffel equation. The group-velocity vector (zero-offset ray) in the first layer is then calculated from the slowness vector. The zero-offset reflection point is found from the traveltime $t_0(1)$, which allows us to compute the depth of the first reflector $z_{\rm calc}^{(1)}$ at the well location. After the first interface has been reconstructed, we repeat the same procedure for the second interface by tracing "back" the zero-offset ray with the slope $p(2)$ (see Grechka *et al.*, 2002b). Continuing this procedure downward yields the estimated reflector depths $z_{\rm calc}^{(n)}$, which can be compared with the measured values.

The interval parameters $V_{P0}^{(n)}, \epsilon^{(n)}, \delta^{(n)}$ are estimated by minimizing the following objective function that contains the differences between the calculated ("calc") and measured quantities:

$$\mathcal{F}(\widetilde{m}) \equiv \sum_{n=1}^{N} \Big(\big\| V_{\rm nmo,calc}(n) - V_{\rm nmo}(n) \big\| + \big\| z_{w,\rm calc}^{(n)} - z_w^{(n)} \big\| + \big\| V_{Gw,\rm calc}^{(n)} - V_{Gw}^{(n)} \big\| \Big) . \tag{29}$$

Grechka *et al.* (2002b) fit only P-wave NMO ellipses in their objective function, because their input data did not include borehole information. Our algorithm operates with 2D data, so we use a single NMO velocity instead of the three parameters of the NMO ellipse. However, we also add two quantities ($z_w^{(n)}$ and $V_{Gw}^{(n)}$) measured from borehole data. Note that the dips $\phi_w^{(n)}$ have been used to constrain the tilt $\nu^{(n)}$ of the symmetry axis in each layer.

For a single layer, the parameter ϵ is constrained only by equations 24 and 25. However, for layered TTI media, $\epsilon^{(n)}$ also contributes to $z_{\rm calc}^{(n)}$ and $V_{\rm nmo,calc}(n)$ (except for $n = 1$). Therefore, although we established that $\epsilon^{(n)}$ cannot be resolved from conventional-spread P-wave data for dips smaller than 60°, it has to be estimated together with $V_{P0}^{(n)}$ and $\delta^{(n)}$. This tomographic inversion can be applied to a single CMP since each layer is laterally homogeneous with planar boundaries.

It should be emphasized that we invert for all interval parameters simultaneously without employing layer

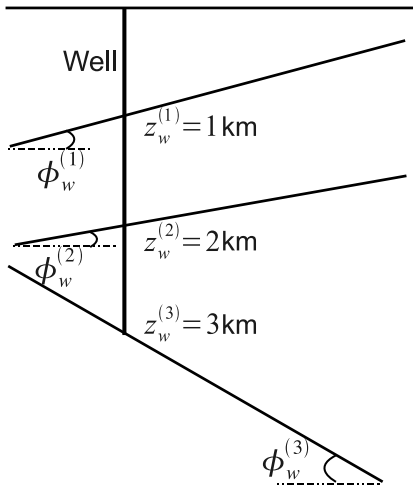

Figure 5. Three-layer TTI model used to test the tomographic algorithm. The dips are $\phi_w^{(1)} = 15^\circ$, $\phi_w^{(2)} = 10^\circ$, and $\phi_w^{(3)} = -30^\circ$. The reflector depths at the well location are $z_w^{(1)} = 1$ km, $z_w^{(2)} = 2$ km, and $z_w^{(3)} = 3$ km.

stripping. This feature of the algorithm helps to reduce error accumulation with depth and is particularly beneficial when the model includes a layer at depth that is known to be isotropic. Then, as demonstrated by Grechka *et al.* (2001) on physical-modeling data for a bending TTI thrust sheet, the reflection from the bottom of the isotropic layer provides valuable constraints on the parameters of the TTI overburden.

3.2 Synthetic example

The algorithm was tested on a three-layer TTI model with dipping interfaces (Figure 5) and the interval parameters listed in Table 4. The inversion results for 200 realizations of noise-contaminated input data are shown in Figure 6. Since the dips are moderate, estimation of the interval parameter ϵ is highly unstable, while V_{P0} and δ can be recovered with sufficiently high accuracy. The standard deviations in the estimated parameters are higher in the third layer (about 2% for V_{P0}, and 0.04 for δ). This reduction in accuracy is due primarily to error accumulation with depth and the smaller contribution of the deeper layers to the effective reflection traveltimes. As was the case for a single layer, rotating the symmetry axis by $\pm 5^\circ$ from the reflector normal does not substantially distort the estimates of V_{P0} and δ.

	Layer 1	Layer 2	Layer 3
V_{P0} (km/s)	1.5	2.0	2.5
ϵ	0.10	0.50	0.25
δ	-0.10	0.30	0.10
ν ($^\circ$)	15	10	-30

Table 4. Interval parameters of the three-layer TTI model from Figure 5. The symmetry axis in each layer is orthogonal to its lower boundary. The input data were distorted by Gaussian noise with the standard deviations equal to 1% for $t_0(n)$ and $p(n)$ and 2% for V_{nmo} and V_{Gw}.

4 DISCUSSION AND CONCLUSIONS

P-wave reflection traveltimes typically do not contain enough information for estimating the parameters of tilted TI models and performing depth imaging. Here, we presented a 2D inversion algorithm for TTI media that supplements P-wave NMO velocities, zero-offset traveltimes, and reflection time slopes with borehole data. It was assumed that borehole measurements provide the vertical group velocity (e.g., from check shots) along with the depths and dips of layer boundaries.

The inversion for a single TTI layer above a dipping reflector (the symmetry axis is confined to dip plane) was based on exact expressions for the phase, group, and NMO velocities. Although the input data allow us to construct enough equations for the symmetry-direction velocity V_{P0}, anisotropy parameters ϵ and δ, and the tilt ν of the symmetry axis, synthetic tests proved the inversion procedure to be highly unstable. Since this problem is caused primarily by an unknown tilt ν, we fixed the symmetry axis in the direction orthogonal to the reflector. This common constraint made it possible to estimate the parameters V_{P0} and δ with high accuracy for the full range of reflector dips. If the magnitude of anisotropy is not uncommonly large ($|\epsilon| \le 0.5$; $|\delta| \le 0.3$) and the dip does not exceed 50°, the algorithm can tolerate the deviation of the symmetry axis from the reflector normal by $\pm 5^\circ$. Stable inversion for the parameter ϵ, however, requires steep dips reaching at least 60°.

To perform interval parameter estimation for a stack of TTI layers separated by plane dipping interfaces, we employed stacking-velocity tomography that operates with conventional-spread P-wave moveout. The current implementation is limited to the 2D model, in which the vertical incidence plane coincides with the dip planes of all interfaces. The symmetry axis is orthogonal to the bottom of each layer, so the tilt ν is known from reflector dips estimated in the borehole. The objective function, computed by ray tracing in a trial model, includes the NMO velocity and two more borehole measurements – the vertical group velocity and

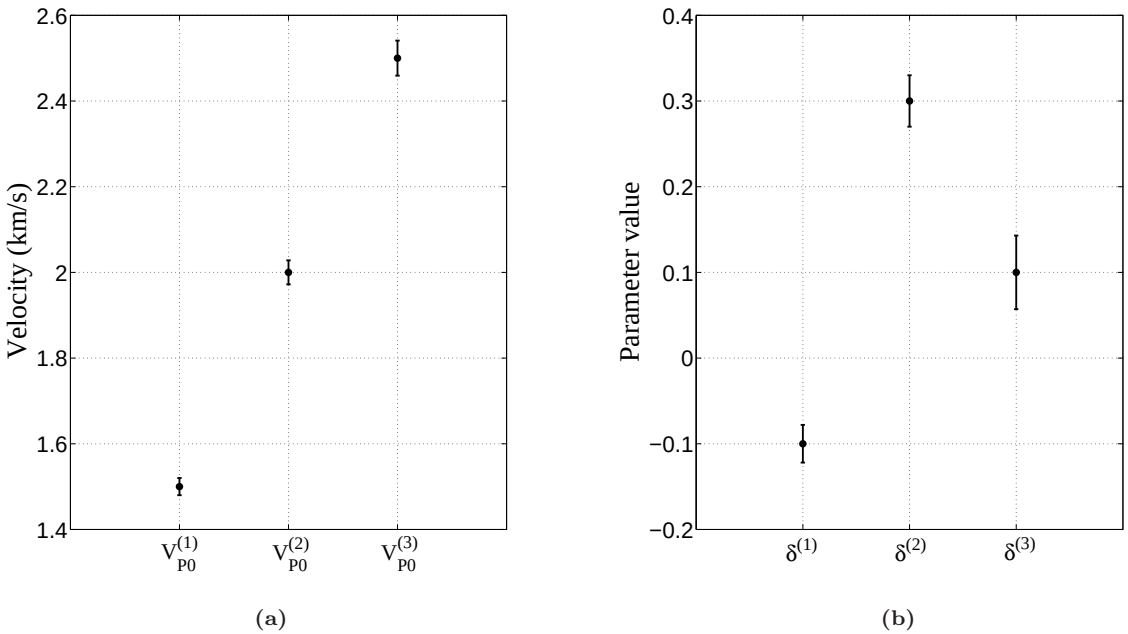

Figure 6. a) Interval symmetry-direction velocities $V_{P0}^{(n)}$ and b) anisotropy parameters $\delta^{(n)}$ $(n = 1, 2, 3)$ estimated by the tomographic inversion for the model from Figure 5 and Table 4. The dots mark the exact values, and the bars correspond to the $\pm$ standard deviation in each parameter.

reflector depth. By performing the inversion for all layers simultaneously, the algorithm mitigates error accumulation with depth. As is the case for a single layer, V_{P0} and δ are well-resolved, while ϵ is poorly constrained for small and moderate reflector dips. If long-spread P-wave data are available, ϵ can be obtained from nonhyperbolic moveout inversion.

Our algorithm can be extended in a straightforward way to 3D wide-azimuth P-wave data by replacing the NMO velocities in the objective function with the NMO ellipses. If the dip and strike of each reflector are measured in the borehole, the orientation of the symmetry axis in each layer is known. Therefore, wide-azimuth data provide additional information for estimating the same interval TTI parameters (V_{P0}, ϵ, and δ), which should enhance the stability of the inversion procedure and reduce errors caused by the deviation of the symmetry axis from the reflector normal.

Stacking-velocity tomography, possibly supplemented with nonhyperbolic moveout inversion for ϵ, represents an efficient tool for building an initial model for migration velocity analysis (MVA) and post-migration reflection tomography. After carrying out the interval parameter estimation at well locations, the V_{P0}- and δ-fields can be computed by interpolation between the wells. An accurate initial TTI model is critically important to ensure the convergence of MVA-based algorithms.

5 ACKNOWLEDGMENTS

We are grateful to Andrey Bakulin (WesternGeco), Paul Fowler (WesternGeco), Vladimir Grechka (Shell), and Andres Pech (IPN, Mexico) for making available their codes and numerous helpful suggestions. We are also grateful to our colleagues from the Center for Wave Phenomena (CWP) for valuable discussions and technical help. This work was supported by the Consortium Project on Seismic Inverse Methods for Complex Structures at CWP.

References

Alkhalifah, T., & Larner, K. 1994. Migration error in transversely isotropic media. *Geophysics*, **59**, 1405–1418.

Alkhalifah, T., Tsvankin, I., Larner, K., & Toldi, J. 1996. Velocity analysis and imaging in transversely isotropic media: Methodology and a case study. *The Leading Edge*, **15**, 371–378.

Behera, L., & Tsvankin, I. 2009. Migration velocity analysis for tilted TI media. *Geophysical Prospecting*, **57**, 13–26.

Charles, S., Mitchell, D. R., Holt, R. A., Lin, J., & Mathewson, J. 2008. Data-driven tomographic velocity analysis in tilted transversely isotropic media: A 3D case history from the Canadian Foothills. *Geophysics*, **73**, VE261–VE268.

Dewangan, P., & Tsvankin, I. 2006a. Modeling and inversion of PS-wave moveout asymmetry for tilted TI media: Part I – Horizontal TTI layer. *Geophysics*, **71**, D107–D121.

Dewangan, P., & Tsvankin, I. 2006b. Modeling and inversion of PS-wave moveout asymmetry for tilted TI media: Part II – Dipping TTI layer. *Geophysics*, **71**, D123–D134.

Grechka, V., & Dewangan, P. 2003. Generation and processing of pseudo-shear-wave data: Theory and case study. *Geophysics*, **68**, 1807–1816.

Grechka, V., & Tsvankin, I. 2000. Inversion of azimuthally dependent NMO velocity in transversely isotropic media with a tilted axis of symmetry. *Geophysics*, **65**, 232–246.

Grechka, V., & Tsvankin, I. 2002. PP+PS=SS. *Geophysics*, **67**, 1961–1971.

Grechka, V., Pech, A., Tsvankin, I., & Han, B. 2001. Velocity analysis for tilted transversely isotropic media: A physical-modeling example. *Geophysics*, **66**, 904–910.

Grechka, V., Pech, A., & Tsvankin, I. 2002a. Multicomponent stacking-velocity tomography for transversely isotropic media. *Geophysics*, **67**, 1564–1574.

Grechka, V., Pech, A., & Tsvankin, I. 2002b. P-wave stacking-velocity tomography for VTI media. *Geophys. Prosp.*, **50**, 151–168.

Huang, T., Xu, S., Wang, J., Ionescu, G., & Richardson, M. 2008. The benefit of TTI tomography for dual azimuth data in Gulf of Mexico. *SEG Expanded Abstracts*, **27**, 222–226.

Isaac, J. H., & Lawton, D. C. 1999. Image mispositioning due to dipping TI media: A physical seismic modeling study. *Geophysics*, **64**, 1230–1238.

Sexton, P., & Williamson, P. 1998. 3D anisotropic velocity estimation by model-based inversion of prestack traveltimes. *SEG Expanded Abstracts*, **17**, 1855–1858.

Thomsen, L. 1986. Weak elastic anisotropy. *Geophysics*, **51**, 1954–1966.

Tsvankin, I. 1996. P-wave signatures and notation for transversely isotropic media: An overview. *Geophysics*, **61**, 467–483.

Tsvankin, I. 2005. *Seismic signatures and analysis of reflection data in anisotropic media, 2nd edition*. Elsevier Science Publ. Co., Inc.

Tsvankin, I., & Grechka, V. 2000. Dip moveout of converted waves and parameter estimation in transversely isotropic media. *Geophys. Prosp.*, **48**, 257–292.

Vestrum, R., Lawton, D. C., & Schmid, R. 1999. Imaging structures below dipping TI media. *Geophysics*, **64**, 1239–1246.

Zhou, B., Greenhalgh, S., & Green, A. 2008. Nonlinear traveltime inversion scheme for crosshole seismic tomography in titled transversely isotropic media. *Geophysics*, **73**, D17–D33.